Melt-Welding and Improved Electrical Conductivity of Nonwoven Porous Nanofiber Mats of Poly(3,4-ethylenedioxythiophene) Grown on Electrospun Polystyrene Fiber Template

Sujith Nair,† Erik Hsiao, and Seong H. Kim*

Department of Chemical Engineering, The Pennsylvania State University, University Park, Pennsylvania 16802

Received August 21, 2008. Revised Manuscript Received November 18, 2008

A simple and efficient way of synthesizing conducting polymers on polymer templates and subsequently improving the connectivity between fibers and hence improving the electrical conductivity of nonwoven porous conducting polymer nanofiber mats is reported. The poly(3,4-ethylenedioxythiophene) (PEDOT) conducting polymer was grown via a vapor-phase polymerization on a nonwoven porous mat of polystyrene (PS) nanofibers containing ferric p-toluenesulfonate (Fe-TS). The PS/Fe-TS nanofibers of diameter ∼300 nm were electrospun and exposed to 3,4-ethylenedioxythiophene (EDOT) vapors. Two different vapor exposure conditions were studied. The shape of the PS template fibers is preserved best under the vapor exposure condition where the EDOT vapor does not condense on the fiber surface. A better electrical conductivity of the fiber mat can be obtained by condensing the EDOT vapor on the PS template fiber during the polymerization. This allows melt-welding of the fibers, which results in a better connectivity between the fibers. The porous PS-PDEOT fiber mats produced under the melt-welding condition showed a sheet conductivity of ∼1 S/cm.

1. Introduction

Conducting polymer nanofibers have drawn much attention from both a fundamental science and an application point of view. There are a number of publications characterizing electrical conduction of individual conducting polymer nanofibers and their applications for sensing.[1−4] However, handling individual nanowires could pose some challenges in practical applications. Apart from these individual nanofiber studies, many researchers have investigated production of conducting polymer nanofibers in large quantities and use them as a platform for electrochemical reactions and sensing.[5−7] The nanofibers collected on solid substrates typically form porous mats consisting of entangled fibers. The porous nanofiber mats can provide high surface areas for sensing element loading and easy transports of analytes across the mats.[8−12]

Various ways of making porous nanofiber mats of conducting polymers have been demonstrated in the literature. These include polymerization in hollow templates, growth on micellar templates, seeded growth, and interfacial polymerizations.[13−21] Recently, an electrospinning technique has been employed to make conducting polymer nanofiber mats.[22−24] The use of electrospinning process may provide several advantages. Various types of polymeric materials can be processed into nanofibers using this method. Porous nanofiber mats can directly be made on various substrates in either random or oriented fashions.[25,26]

* Corresponding author. E-mail: shkim@engr.psu.edu.
† Current address: Milliken & Company, Spartanburg, SC 29304.

(1) Liu, L.; Jia, N.-G.; Zhou, Q.; Yan, M.; Jiang, Z.-Y. *Mater. Sci. Eng., C* **2007**, *27*, 57.
(2) Wanekaya, A. K.; Bangar, M. A.; Yun, M.; Chen, W.; Myung, N. V.; Mulchandani, A. *J. Phys. Chem. C* **2007**, *111*, 5218.
(3) Shen, J.; Chen, Z.; Wang, N.; Yan, H.; Shi, G.; Jui, A.; Gu, C. *Appl. Phys. Lett.* **2006**, *88*, 253106.
(4) Raynes, O.; Demoustier-Champagne, S. *J. Electrochem. Soc.* **2005**, *152*, D130.
(5) Zhang, X.; Wang, J.; Wang, Z.; Wang, S. C. *J. Macromol. Sci., Part B: Phys.* **2006**, *45*, 475.
(6) Potje-Kamloth, K. *Crit. Rev. Anal. Chem.* **2002**, *32*, 121.
(7) Brahim, S.; Narinesingh, D.; Guiseppi-Elie, A. *Biosens. Bioelectron.* **2002**, *17*, 53.
(8) Kenawy, E. K.; Bowlin, G. L.; Mansfield, K.; Layman, J.; Simpson, D. G.; Sanders, E. H.; Wrek, G. E. *J. Controlled Release* **2002**, *81*, 57.
(9) Li, W. J.; Laurencin, C. T.; Caterson, E. J.; Tuan, R. S.; Ko, F. K. *J. Biomed. Mater. Res.* **2002**, *60*, 613.
(10) Herricks, T. E.; Kim, S.-H.; Kim, J.; Li, D.; Kwak, J. H.; Grate, J. W.; Kim, S. H.; Xia, Y. *J. Mater. Chem.* **2005**, *15*, 3241.
(11) Kim, B. C.; Nair, S.; Kim, J.; Kwak, J. H.; Grate, J. W.; Kim, S. H.; Gu, M. B. *Nanotechnology* **2005**, *16*, S82.
(12) Nair, S.; Kim, J.; Crawford, B.; Kim, S. H. *Biomacromolecules* **2007**, *8*, 1266.
(13) Samitsu, S.; Iida, T.; Fujimori, M.; Heike, S.; Hashizume, T.; Shimomura, T.; Ito, K. *Synth. Met.* **2005**, *152*, 497.
(14) Duvail, J. H.; Retho, P.; Garreau, S.; Louarn, G.; Godon, C.; Champagne, D.-S. *Synth. Met.* **2002**, *131*, 123.
(15) Han, M. G.; Foulger, S. H. *Chem. Commun.* **2005**, 3092.
(16) Xinyu, Z.; Lee, J.-S.; Lee, G. S.; Cha, D.-K.; Kim, M. J.; Yang, D. J.; Manohar, S. K. *Macromolecules* **2006**, *39*, 470.
(17) Han, M. G.; Foulger, S. H. *Small* **2006**, *2*, 1164.
(18) Kim, B. H.; Park, D. H.; Joo, J.; Yu, S. G.; Loe, S. H. *Synth. Met.* **2005**, *150*, 279.
(19) Zhang, X.; Goux, W. J.; Manohar, S. K. *J. Am. Chem. Soc.* **2004**, *126*, 4502.
(20) Zhang, X.; Manohar, S. K. *J. Am. Chem. Soc.* **2004**, *126*, 12714.
(21) Huang, J.; Kaner, R. B. *J. Am. Chem. Soc.* **2004**, *126*, 851.
(22) Liu, H. Q.; Kameoka, J.; Czaplewski, D. A.; Craighead, H. G. *Nano Lett.* **2004**, *4*, 671.
(23) MacDiarmid, A. G.; Jones, W. E.; Norris, I. D.; Gao, J.; Johnson, A. T.; Pinto, N. J.; Hone, J.; Han, B.; Ko, F. K.; Okuzaki, H.; Llaguno, M. *Synth. Met.* **2001**, *119*, 27.
(24) Nair, S.; Natarajan, S.; Kim, S. H. *Macromol. Rapid Commun.* **2005**, *26*, 1599.
(25) Li, D.; Wang, Y.; Xia, Y. *Nano Lett.* **2003**, *3*, 1167.

10.1021/cm8029449 CCC: $40.75
Published on Web 12/16/2008

The first application example of the electrospinning method to fabrication of conducting polymer nanofibers was the fabrication of polyaniline composite nanofibers.[22,23] In this case, polyaniline was dissolved in other polymer matrix solutions and electrospun into nanofibers. One of the reasons to make polyaniline nanofibers in a composite form is that the molecular weight of polyaniline itself is not high enough to create extensive chain entanglements needed to form fibers after solvent evaporation from electrospun polymer solution jets. Electrospinning is typically done with high-molecular-weight polymers (typically greater than 1×10^5 amu). In the case of electrospinning of nanofibers from polymer mixture solutions, the choice and amount of matrix polymer is critical. If the conducting polymer portion is too small, the produced fiber mat would not have electrical conductivity. If the matrix polymer portion is too small, the electrospinning of nanofibers would be difficult. Another requirement is that the conducting polymer should be soluble in solvent; otherwise, it cannot be processed into fibers with the electrospinning technique.

These challenges in electrospinning of conducting polymers in a composite form can be avoided if conducting polymers are produced directly on electrospun porous nanofiber mat templates. Two methods can be used to grow conducting polymers on porous material surfaces. One is the chemical vapor deposition.[27,28] In this technique, the oxidant and monomer vapors are simultaneously deposited to the template surface. The other is a vapor phase polymerization. In this process, template substrates containing Fe(III) oxidants are produced first and then exposed to the monomer vapor. The polymerization occurs upon the absorption and diffusion of the monomer into the template surface.[29−31] We have demonstrated application of the vapor phase polymerization to electrospun template fibers to grow polyporrole (PPy) layers.[24,32] Although the vapor phase polymerization is known to achieve a conductivity of higher than 100 S/cm,[29−33] the sheet electrical conductivity of the PPy-coated porous nanofiber mats was in the range of 1×10^{-4} to 1×10^{-2} S/cm. It is believed that the poor connectivity between nanofibers appears to limit the sheet conductivity of the porous fiber mat.

In this paper, we report the enhancement of sheet conductivity of the porous conducting polymer nanofiber mats. Polystyrene was chosen as a template material. Conducting polymer fabricated on hydrophobic polystyrene matrices could be used in aqueous solutions for sensing purposes without disruption of the matrix. Also, the electrospinning of polystyrene and the issues associated with it have been well-documented in the literature. Poly-3,4-ethylenedioxythiophene (PEDOT) was chosen in this study because the side-chain interactions in PEDOT induced ordering of the π-conjugated backbone into a crystalline phase, giving rise to a better conductivity than the amorphous polymers.[34−37] In addition, PEDOT has good environmental stability needed for various practical applications.[38−40] The fabrication process consists of two steps - electrospinning of polystyrene (PS) template nanofibers that contain ferric p-toluenesulfonate (FeTS) followed by vapor-phase polymerization of 3,4-ethylenedioxythiophene (EDOT). FeTS is one of the most efficient oxidants for EDOT polymerization and produces intrinsically doped and electrically conducting PEDOT.[35,36] To increase the connectivity of the porous PS-PEDOT nanofiber mat, we can melt-weld the nanofibers during the vapor-phase polymerization by condensing the EDOT monomer on the template fiber. The controlled condensation of EDOT partially dissolves the PS nanofibers, causing welding of the PS nanofibers while keeping the pores of the nonwoven fiber mat. With this approach, a porous PS-PEDOT nanofiber mat with a sheet electrical conductivity of ~1 S/cm can be obtained.

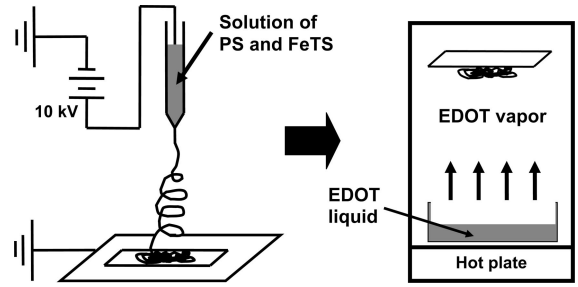

Figure 1. Schematic of the electrospinning of PS-PSMA-FeTS nanofiber templates and vapor phase polymerization of EDOT. Both the substrate and the EDOT are heated to 70 °C.

2. Experimental Section

2.1. Electrospinning of PS-FeTS Nanofibers. The PS-PEDOT nanofibers were prepared by electrospinning a solution of PS (molecular weight ~350 000 amu) and FeTS (40 wt % FeTS in butanol, Baytron-C) in a tetrahydrofuran (THF)-acetone-butanol solvent system, followed by exposure to the vapor of EDOT at 70 °C. Schematic of electrospinning and vapor phase polymerization is shown in Figure 1. The PS solution for electrospinning was prepared by dissolving a 3:1 mixture of PS and poly (styrene-co-maleic anhydride) (PSMA; molecular weight ~224 000 amu; maleic anhydride fraction = 7%) in THF. The use of PSMA in the PS electrospinning is to reduce bead defect formation in nanofibers during the electrospinning.[10−12,24,32,41] A 1:1 mixture (by weight) of FeTS solution (Baytron-C) and acetone was added to the THF solution of PS and PSMA. The total FeTS in the mixture was ~5 wt % and the total concentration of the solid (polymer and oxidant)

(26) Li, D.; Xia, Y. *Nano Lett.* **2003**, *3*, 555.
(27) Lock, J. P.; Im, S. G.; Gleason, K. K. *Macromolecules* **2006**, *39*, 5326.
(28) Im, S. G.; Olivetti, E. A.; Gleason, K. K. *Surf. Coat. Technol.* **2007**, *201*, 9406.
(29) Winther-Jensen, B.; Breiby, D. W.; West, K. *Synth. Met.* **2005**, *152*, 1.
(30) Winther-Jensen, B.; West, K. *Macromolecules* **2004**, *37*, 4538.
(31) Forrest, S. R. *MRS Bull.* **2005**, *30*, 28.
(32) Nair, S.; Hsiao, E.; Kim, S. H. J. *Mater. Chem* **2008**, *18*, 5155.
(33) Winther-Jensen, B.; Chen, J.; West, K.; Wallace, G. *Macromolecules* **2004**, *37*, 5930.
(34) Skotheim, T. *Handbook of Conducting Polymers*, 2nd ed.; CRC Press: Boca Raton, FL, 1987.
(35) Aasmundtveit, K. E.; Samuelsen, E. J.; Pettersson, L. A. A.; Inganas, O.; Johansson, T.; Feidenhans'l, R. *Synth. Met.* **1999**, *101*, 561.
(36) Kine, R. J.; McGehee, M. D. *Polym. Rev.* **2006**, *46*, 27.
(37) Aleshin, A. W.; Sandberg, H.; Stubb, H. *Synth. Met.* **2001**, *121*, 1449.
(38) Granstrom, M.; Berggren, M.; Inganas, O. *Science* **1995**, *267*, 1479.
(39) Roncali, J. *Chem. Rev.* **1992**, *92*, 711.
(40) McCullogh, R. In *Handbook of Oligothiophenes and Polythiophenes*; Fichou, D., Ed.; Wiley-VCH: Weinheim, Germany, 1999.
(41) Megelski, S.; Stephens, J. S.; Chase, D. B.; Rabolt, J. F. *Macromolecules* **2002**, *35*, 8456.

was ~15 wt %. The PS-FeTS solution was then loaded in a glass pipet with a tip diameter of about 200−400 μm. An inert electrode (nickel−chromium wire) was placed into the glass pipet loaded with the polymer solution and a positive bias of ~10 kV was applied to the solution using a high voltage supply. The as-spun PS-FeTS template fibers were collected on a grounded electrode (aluminum foils or glass slides) placed ~7 cm from the glass pipet tip.

2.2. Vapor-Phase Polymerization of EDOT on PS-FeTS Nanofibers. The electrospun PS-FeTS fibers were exposed to EDOT vapors at 70 °C. To avoid condensation of the vapors the substrate containing the PS-FeTS nanofibers were kept at 70 °C. The EDOT vapor exposure times varied from ~5 min to 6 h.

2.3. Melt-Welding of PEDOT Nanofiber Mats. Melt-welded PEDOT nanofiber mats were produced by condensing the EDOT vapor onto substrates containing the PS-FeTS fibers. The EDOT vapors were generated by heating a liquid reservoir to ~70 °C in the reactor unit while the PS-FeTS fibers were kept at ~35 °C. The condensation times varied from ~5 min to 6 h. For all analysis purposes, the samples were dried overnight in a vacuum oven.

2.4. Characterization of the PEDOT Nanofibers. The morphology of the PS-PEDOT fibers was characterized using field emission scanning electron microscopy. For FE-SEM imaging, a thin layer of iridium (~2 nm) was sputter-coated onto the sample to prevent charging problems. The vapor phase polymerization of EDOT on the electrospun PS-FeTS template fibers was monitored as a function of EDOT vapor exposure time using transmission Fourier transform infrared spectroscopy (FTIR). Vibrational spectra of the samples were obtained in the range from 400 to 4000 cm^{-1} with a 4 cm^{-1} resolution. The crystalline phase in the PS-PEDOT fibers was characterized using X-ray diffraction (XRD; X-ray source = Cu Kα radiation). A four-probe conductivity of the as-polymerized nonwoven nanofiber mats of PS-PEDOT was measured at various times of polymerization by the van der Pauw method. For conductivity measurements, the PS-PEDOT nanofiber mats were produced on 1 cm × 1 cm glass slides. Electrical contacts were made at the four corners of the sample using a silver paint. The nominal thickness of the samples needed for conductivity calculation was measured with cross-sectional FE-SEM.

3. Results and Discussion

3.1. Electrospinning of PS-FeTS Nanofibers. It is important to obtain high-quality template nanofibers at the first place because the conducting polymer is grown on these template fibers. One of the controlling factors in the electrospinning of PS-FeTS was the choice of solvent. The solvent should be able to dissolve both PS polymer and FeTS salt and have a proper vapor pressure. For electrospinning of PS, THF was known to be a good solvent.[10−12,41] But the FeTS solution does not mix with THF. It was found that adding 16−32 wt % acetone to THF prevents phase separation during mixing of FeTS and PS. Because acetone and THF have vapor pressures higher than butanol, they will evaporate faster than butanol during solvent evaporation from the electrospun polymer solution jet. Since PS does not dissolve in butanol, it could be segregated from the FeTS-butanol phase at the last moment of the electrospun jet drying. The butanol added to the system from the FeTS stock solution also improved the stability of the electrospinning process and allowed continuous production of PS-FeTS nanofibers.

The maximum amount of FeTS incorporated into the electrospinning solution was ~5 wt %. If the FeTS amount was higher than 5 wt %, the solution becomes too viscous for electrospinning. The as-spun PS-FeTS fibers had the characteristic yellowish color of the Fe (III) salt. When the electrospun PS-FeTS nanofibers were exposed to EDOT vapor at 70 °C, the nanofiber color changed to the characteristic blue color of PEDOT.[42]

3.2. Vapor-Phase Polymerization of PEDOT on PS-FeTS Nanofibers. The high resolution FE-SEM images of the PS-FeTS template fibers and the vapor-phase polymerized PS-PEDOT fibers are shown in Figure 2. The as-spun PS-FeTS template fibers showed a smooth morphology on the polymer fiber surface (images a and b in Figure 2). The fiber diameters were found to be 300 ± 60 nm. The nanofiber structure was preserved during the vapor phase polymerization (Figures 2c−f). The high resolution FE-SEM images of the PS-PEDOT nanofibers show small platelets at the surface. No noticeable increase in the nanofiber diameter distribution size was observed after the vapor polymerization of EDOT. During the polymerization, the FeTS oxidant is reduced to Fe(II) species that can be washed out by proper solvents. However, rigorous washing could lead to disruption of the nanofiber structure. To preserve the integrity of the nanofiber matrix, we did not attempt to wash to remove the excess Fe(II).

The ordering of PEDOT chains into a crystalline form can result in a good charge carrier transport property.[35] Figure 3 displays the XRD patterns of PS-FeTS and PS-PEDOT nanofibers. In the case of PS-FeTS, only one broad peak centered at $2\theta \approx 19°$ was observed, which could be attributed to the amorphous phase of PS. As the PEDOT phase grew through the vapor phase polymerization of EDOT, crystalline peaks at $2\theta = 6.4°$ (d-spacing = 13.7Å) and 18.3° (d-spacing = 4.8Å) were increased. These peaks correspond to the [100] and [020] planes of the PEDOT orthorhombic unit cell, respectively.[35,43,44] These results implied the presence of crystalline PEDOT domains in the PS-PEDOT nanofibers.

The PEDOT growth was monitored as a function of polymerization time. Initially, a gravimetric weighing method was employed to measure the absolute amount of the PEDOT produced; but it did not work well because the PEDOT amount produced via vapor-phase polymerization was too small. Another potential method that might be used to determine the mass gain during the conducting polymer growth would be a quartz crystal microbalance (QCM) technique. However, our previous study of pyrrole polymerization over electrospun polyethyleneoxide template fibers found that the QCM frequency response cannot be correlated directly to the mass uptake by the conventional Saurbrey equation because of changes in the stiffness and viscoelastic properties of the fibers.[24] In this experiment, the growth of PEDOT was monitored spectroscopically using FTIR. Although the absolute amount of the polymer produced cannot be measured, this method allows us to determine the relative

(42) Pei, Q.; Zuccarello, G.; Ahlskog, M.; Inganas, O. *Polymer* **1994**, *35*, 1347. (a) Pei, Q.; Zuccarello, G.; Ahlskog, M.; Inganas, O. *Polymer* **1994**, *35*, 1347.
(43) Aasmundtveit, K. E.; Samuelsen, E. J.; Inganas, O.; Pettersson, L. A. A.; Johansson, T. *Synth. Met.* **2000**, *113*, 93.
(44) Hsu, F.-C.; Prigodin, V. N.; Epstein, A. J. *Phys. Rev. B* **2006**, *74*, 235219.

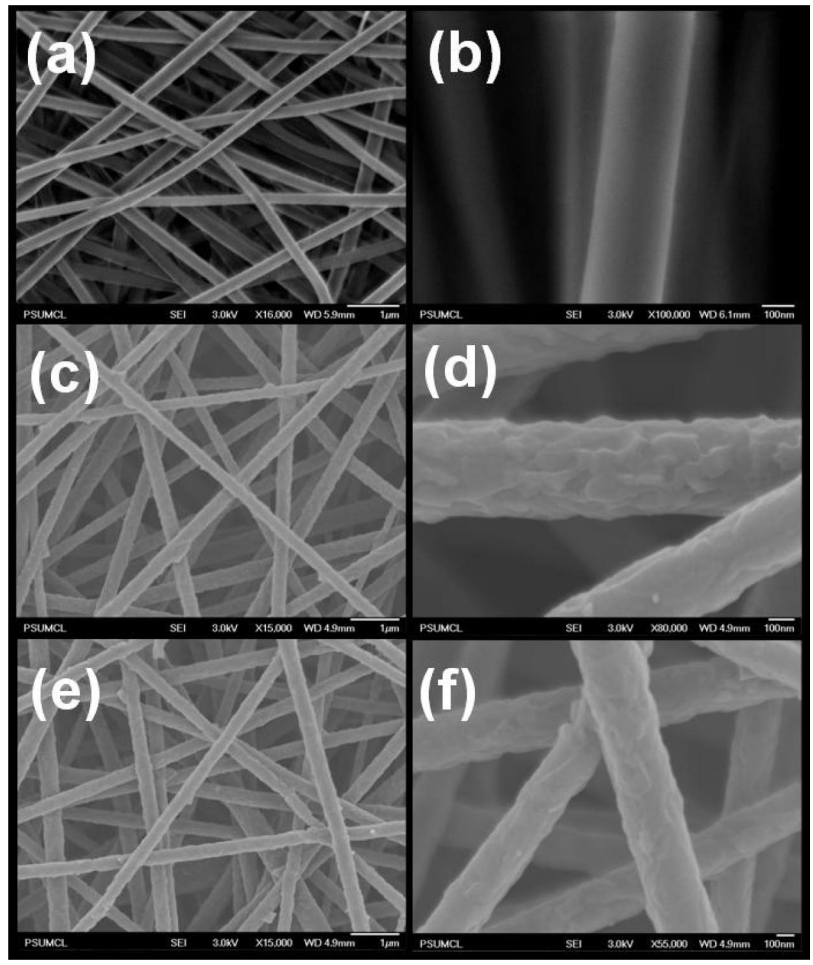

Figure 2. FESEM image of PS-PEDOT nanofibers obtained by exposing (a, b) PS-FeTS fibers to EDOT vapors at 70 °C for (c, d) 1 and (e, f) 6 h.

amount of the PEDOT product at a given time with respect to the maximum amount produced after a long polymerization time.

Figure 4 shows FTIR spectra of the as-spun PS-FeTS template fibers and PS-PEDOT nanofibers produced after 1, 3, and 6 h of EDOT vapor polymerization. In the case of PS-FeTS, the FTIR spectrum was dominated by the characteristic bands of PS, maleic anhydride, and the p-toluenesulfonate anion. The PS peaks were the C−H stretching within the aromatic ring in the 3000∼3100 cm^{-1} region, the C−H deformation in the aromatic ring at 1450 and 1490 cm^{-1}, the C═C ring stretching in the aromatic ring at 1605 cm^{-1}, and the aromatic overtones in the 1700 ∼ 2000 cm^{-1} range. The peaks at 1780 cm^{-1} and 1850 cm^{-1} were symmetric and asymmetric C═O stretching of the maleic anhydride group. The peaks at 1035 and 1008 cm^{-1} are attributed to the sulfonyl group of the toluenesulfonate anion. Upon exposure to the EDOT vapor, the vibrational bands of PEDOT grew and became dominant. These peaks included the symmetric and asymmetric C−H stretching of the ethylene group in PEDOT at 2852 and 2920 cm^{-1}, respectively; the C−H bending of the ethylene group at 1449 and 1464 cm^{-1}; the C−O−C stretching at 1237 and 1185 cm^{-1}; the C═C stretching in the thiophene ring at 1370 cm^{-1}; and the C−S ring stretching at 935, 840 and 605 cm^{-1}. The increase of the baseline above 2000 cm^{-1} implied that the produced PEDOT is electrically doped.[45] The peak at 1750 cm^{-1} can be attributed to the C═O species. This species could be produced if conducting polymer chains are overoxidized by the oxidant present nearby. Another possible side reaction is the cleavage and oxidation of the dioxane group in the monomer.[30] These side reactions may result in a nonconducting material.

Figure 5 plots the intensity of 1237 cm^{-1} (one of the strongest PEDOT IR peaks) versus vapor phase polymerization time. The solid line is the fit to a simple diffusion-reaction model.[32,46] The amount of PEDOT produced increases rapidly with the exposure time at the beginning and then levels off after ∼4 h. The polymerization can take place either at the surface of the template nanofibers or in the skin layers of the nanofibers or both. In either case, the diffusion of the EDOT monomer through the PEDOT product layer is required to continue producing the reaction product. This diffusion would get more difficult as the PEDOT layer thickness increases; so, it becomes self-limiting. This self-limited growth thickness is apparently large enough to mask the vibrational peaks of the PS template inside. The formation

(45) Rodriguez, I.; Scharifker, B. R.; Mostany, J. *J. Electroanal. Chem.* **2000**, *491*, 117.
(46) Smith, J. M. *Chemical Engineering Kinetics*, 3rd ed.; McGraw-Hill: Columbus, OH, 1981.

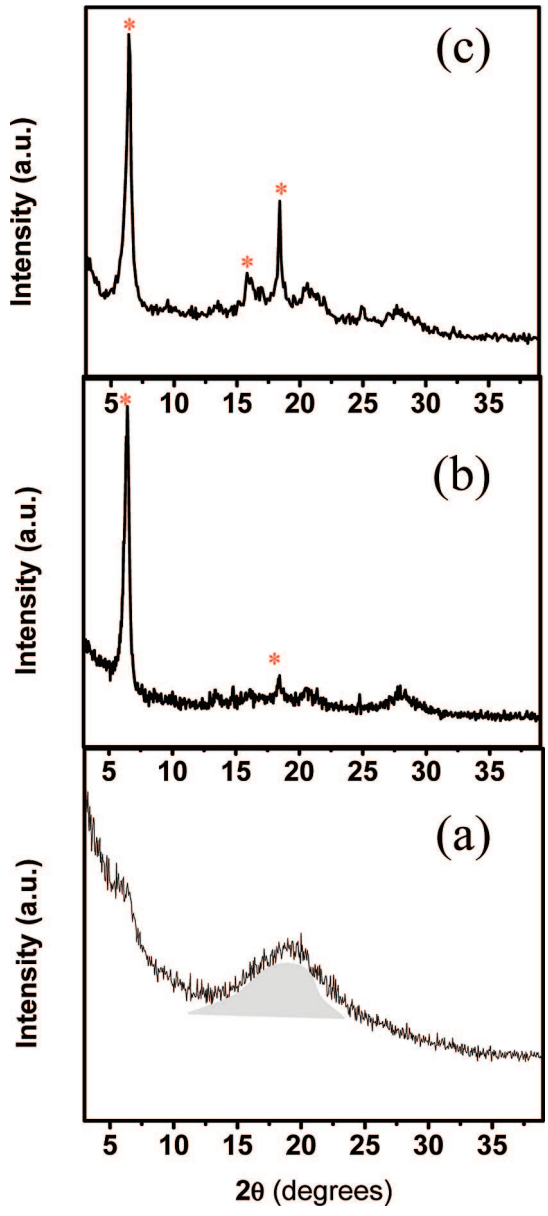

Figure 3. XRD of PS-FeTS fibers monitored as a function of time of exposure to EDOT vapors (a) as-spun PS-FeTS fibers, (b) PS-FeTS fibers exposed to EDOT vapors for 1 h, (c) PS-FeTS fibers exposed to EDOT vapors for 3 h. Crystalline peaks are marked with ∗; amorphous phase background is marked in gray color. During the polymerization, the EDOT vapors and the PS-FeTS fibers are kept at 70 °C.

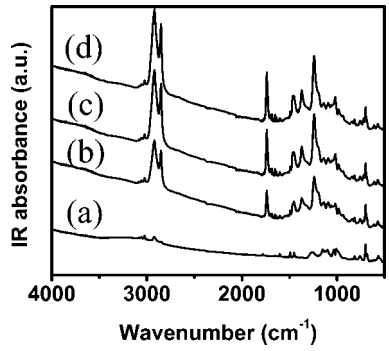

Figure 4. Transmission FTIR spectra of (a) electrospun PS-FeTS fibers and PS-PEDOT nanofibers after vapor polymerization for (b) 1, (c) 3, and (d) 6 h. During the polymerization, the EDOT vapors and the PS-FeTS fibers are kept at 70 °C.

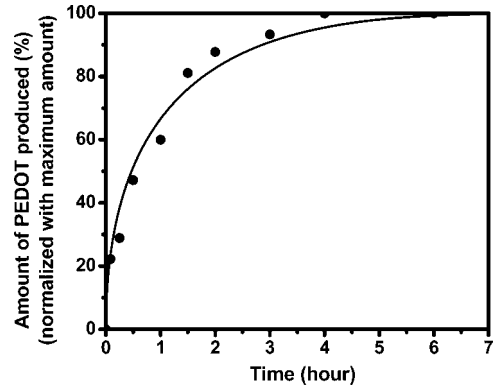

Figure 5. Growth of PEDOT (1237 cm^{-1} FTIR intensity) on PS-FeTS fibers monitored as a function of the EDOT vapor exposure time at 70 °C. The solid line is the fit to a simple diffusion-reaction model.[32,46]

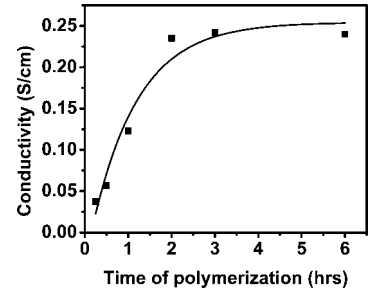

Figure 6. Conductivity of PS-FeTS fibers monitored as a function of time of exposure to EDOT vapors. The conductivities were measured from the Van der Pauw equation. During the polymerization, the EDOT vapors and the PS-FeTS fibers are kept at 70 °C.

of thick surface PEDOT layers is also supported by the platelet-like morphology observed after the vapor-phase polymerization (Figure 2).

Although the FTIR intensity could not be converted to the exact quantity of PEDOT in the sample, it could still be compared with the electrical conductivity. Figure 6 plots the sheet conductivity of the as-produced PS-PEDOT nanofiber mat versus the EDOT exposure time. The increase of electrical conductivity closely follows the PEDOT growth kinetics shown in Figure 5. The sheet conductivity initially increased rapidly with the polymerization time and then leveled off after ∼2 h. This result implies that the electrical conductivity of the PS-PEDOT nanofiber mat is roughly proportional to the amount of PEDOT produced though the vapor-phase polymerization. The maximum sheet conductivity of the PS-PEDOT nanofiber mat reached ∼0.24 S/cm. The conductivity of individual fibers would be much higher than the sheet conductivity of the nanofiber mat since the sheet conductivity was calculated using nominal thickness of the PS-PEDOT fiber mat without considering the presence of insulating core (PS template) and the void volume between the PE-PEDOT nanofibers.

3.3. Melt-Welding of PEDOT Nanofibers. In order to further increase the sheet conductivity of the nonwoven porous nanofiber mats, one could attempt to use more Fe(III) oxidant to produce more PEDOT on the template nanofibers. But, the amount of oxidant that can be incorporated into the template nanofiber is limited by the processibility of template fiber electrospinning. In this situation, the next strategy would be to improve the connectivity between PEDOT nanofibers.

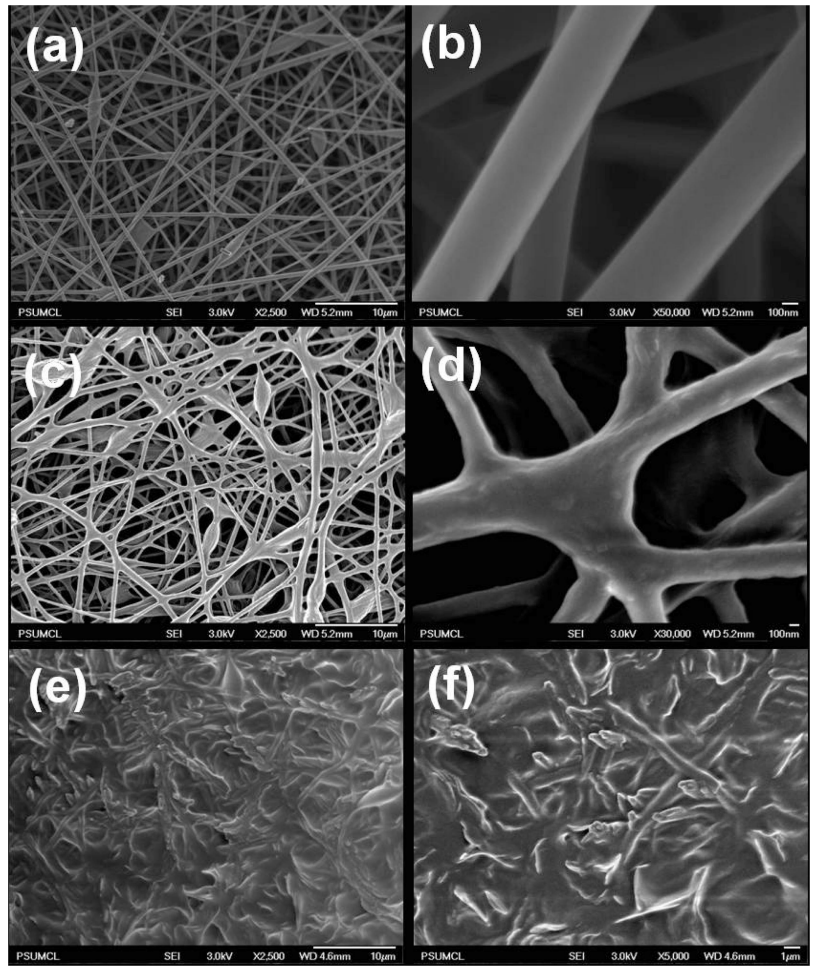

Figure 7. FESEM image of melt-welded PS-PEDOT nanofibers obtained by exposing PS-FeTS nanofibers under the EDOT condensation condition for (a, b) 1, (c, d) 10, and (e, f) 20 min. During the polymerization the EDOT liquid source temperature was 70 °C and the PS-FeTS fiber temperature was kept at 30 °C.

It is well-known that the charge carrier transport in polycrystalline samples is often limited by the grain boundary contacts.[48] The same can be applied to the nonwoven nanofiber mats since the conducting polymer nanofibers are loosely entangled and packed to form porous structures. One way to achieve better connectivity is a photochemical welding of nanofibers in the porous mat by using a high flux light source.[47−49] This method is applicable to polymers with low luminescence efficiency (such as polyaniline) thereby converting most of the absorbed photon energy into heat and melting the nanofibers. This method was attempted for the PS-PEDOT nanofibers, but it did not work. This could be explained by the fact that PEDOT has a high luminescence efficiency, which results in a low conversion of the absorbed photon energy into heat.

Because the PEDOT layer could not be welded once it is produced, the possibility of welding nanofibers during the PEDOT growth was explored. The main idea was to use the solubility of PS in the EDOT liquid. By controlling the amount of the condensed EDOT liquid on the PS-FeTS template nanofibers, one could partially melt and weld the PS fibers. This could also increase the polymerization rate since more EDOT monomers are readily available for polymerization. For the condensation of EDOT vapor onto the temperature of PS-FeTS template nanofibers, the temperature of the fiber mat was lowered to 35 °C during the vapor phase polymerization while keeping the EDOT vapor source (liquid reservoir) at 70 °C. Figure 7 shows the FE-SEM images of PS-PEDOT nanofibers produced under the EDOT condensation condition for 1 min, 10 min, and 20 min. The template nanofiber shape remained intact after 1 min of polymerization. However, it can clearly be seen that after 10 min of polymerization under the EDOT condensation condition, the junction points of PS-PEDOT nanofibers are fused together. If the template fiber is exposed too long to the EDOT liquid condensate, the PS-FeTS template nanofibers can completely melt and form a continuous film without pores. This complete melting can be seen for the ∼20 min exposure sample.

The sheet conductivity of the porous PS-PEDOT nanofiber mats welded through EDOT condensation was plotted as a function of the EDOT condensation-polymerization time (Figure 8). The highest sheet conductivity was observed to be ∼1 S/cm for the 10 min sample in which the PS-PEDOT nanofibers are welded to each other without losing the pores

(47) Huang, J.; Kaner, R. B. *Nat. Mater.* **2004**, *3*, 783.
(48) Ajayan, P. M.; Ramanath, G.; Terrones, M.; Ebbesen, T. W. *Science* **2002**, *297*, 192.
(49) Wang, N.; Yao, B. D.; Chan, Y. F.; Zhang, X. Y. *Nano Lett.* **2003**, *3*, 475.

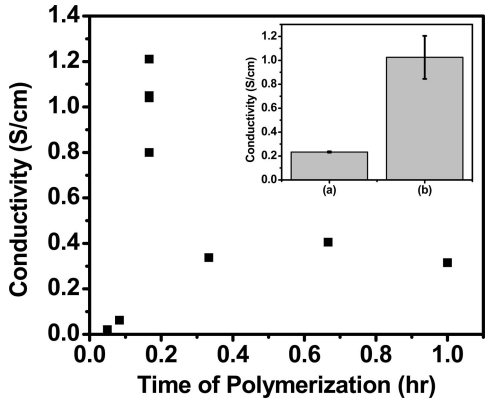

Figure 8. Changes of sheet conductivity of PS-PEDOT nanofiber porous mat as a function of polymerization time under the EDOT condensation conditions (EDOT source temperature = 70 °C and the PS-FeTS fiber temperature = 35 °C). The inset compares the maximum conductivities obtained for (a) vapor-phase polymerized PS-PEDOT fibers without EDOT condensation and (b) melt-welded PS-PEDOT nanofibers.

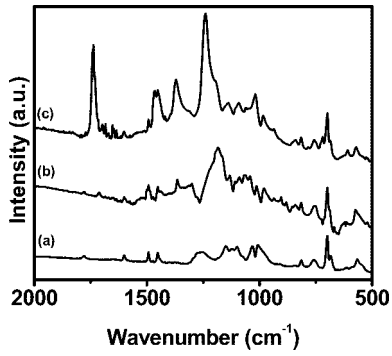

Figure 9. Transmission FTIR spectra of (a) electrospun PS-FeTS fibers and melt-welded PS-PEDOT nanofibers produced after polymerization under the EDOT condensation condition for (b) 10 and (c) 60 min.

between the fibers. This is roughly 4 times higher than the PS-PEDOT nanofibers obtained without the EDOT condensation during the polymerization (Figure 8, inset). When the condensation-polymerization time is increased too long, the sheet conductivity of the PS-PEDOT mat decreases to lower values even the sample morphology changed from the porous structure to the continuous thin film.

The maximum conductivity after 10 min of polymerization under the EDOT condensation condition might be related to the following two factors. In the FTIR analysis (Figure 9), it was found that the 10 min sample does not show the C=O peak at 1750 cm^{-1}, whereas the 60 min sample contains a significant amount of the C=O species. Note that the carbonyl peak might be related to the side reactions of PEDOT polymerization which produce nonconducting or poorly conducting products. The complete melting of the template nanofiber can also lead to dilution of PEDOT in the PS matrix which prevents the crystallization of PEDOT and eventually results in random distribution of conducting polymers within the insulating polymer matrix. Figure 10 compares XRD spectra of the PS-PEDOT produced by polymerization for 10 and 20 min under the EDOT condensation condition. In the case of 10 min condensation/polymerization, the PEDOT produced is still crystalline,

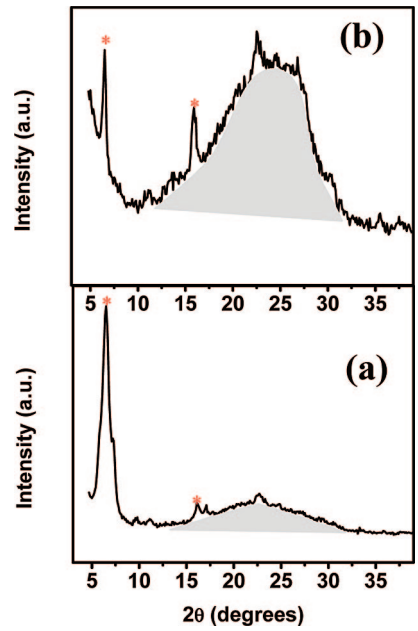

Figure 10. XRD of melt-welded PS-PEDOT nanofibers obtained by exposing PS-FeTS nanofibers to EDOT vapors at 70 °C for (a) exposure time = 10 min and (b) exposure time = 60 min. Crystalline peaks are marked with ∗; amorphous phase background is marked in gray color. During the polymerization, the EDOT vapors are at 70 °C and the PS-FeTS fibers are kept at 35 °C.

showing sharp peaks at $2\theta = 6.4°$ and 18°.[50] However, after 20 min of condensation-polymerization, the crystalline peak intensities are weak and a broad background centered at ~23° is dominating, indicating the presence of a large amount of amorphous phase.

4. Conclusions

The nonwoven porous mat of PS-PEDOT nanofibers with an average diameter of 300 nm was fabricated by a two-step process involving electrospinning of PS-FeTS template fibers followed by exposure to the EDOT vapor at 70 °C. After the vapor phase polymerization, the sheet conductivities of the PS-PEDOT composite nanofiber mats were ~0.24 S/cm. The conductivity of the PEDOT layer on individual nanofibers would be much higher since the sheet conductivity was calculated without taking into account the presence of insulating PS in the fiber and the interfiber pore volume in the nonwoven fiber mat. The sheet conductivity of the porous nanofiber mat could be increased by growing PEDOT under the monomer condensation condition. This caused melt-welding of the PS-PEDOT fibers, improving the connectivity between individual nanofibers. By controlling the condensation of EDOT onto the PS-FeTS template fibers during the PEDOT growth, the welded PS-PEDOT nanofibers were produced while keeping the pore in the nonwoven mat intact. The sheet conductivity of the melt-welded PS-PEDOT nanofiber mat was increased to ~1 S/cm.

Acknowledgment. The authors acknowledge financial support from the National Science Foundation (Grant DMI-0210229).

CM8029449

(50) Hsu, F.-C.; Prigodin, V. N.; Epstein, A. J. *Phys. Rev. B* **2006**, *74*, 235219.